

Investigation of the contact zone of a cylindrical shell located between two parallel rigid plates with a gap

Arseniy V. BABAYTSEV^{*1}, Lev N. RABINSKIY¹, Kyaw Thu AUNG²

*Corresponding author

¹Institute of General Engineering Training,
Moscow Aviation Institute (National Research University),
4 Volokolamskoe Shosse, 125993, Moscow, Russian Federation,
Ar77eny@gmail.com*, rabinskiy@mail.ru

²Marine Electrical System and Electronics - Myannar Navy,
Defence Services Technological Academy (DSTA),
Mandalay-Lashio Highway, Pyin Oo Lwin, Mandalay Division, Myanmar,
koaktmai@gmail.com

DOI: 10.13111/2066-8201.2020.12.S.4

Received: 18 March 2020/ Accepted: 28 May 2020/ Published: July 2020

Copyright © 2020. Published by INCAS. This is an “open access” article under the CC BY-NC-ND license (<http://creativecommons.org/licenses/by-nc-nd/4.0/>)

Abstract: *The article presents the results of a study of the contact zone of a thin-walled cylindrical shell located between two parallel rigid plates. The shell under consideration was located with various gaps from the rigid plate and was subsequently subjected to internal pressure. In the course of such a study, experimental, numerical and analytical estimates of the contact zone width were obtained depending on the discharge pressure. The obtained numerical and analytical estimates are tested with experiment. To study the width of the contact zone, depending on the gap, a testing workbench was used. The problem of numerical and analytical modelling was solved by the finite element analysis in the Ansys Workbench system. The solution to transcendental equation was found numerically using the Newton-Raphson method. As a result of experimental, numerical and analytical studies, results were obtained for a plane-oval shell with gaps of 0.5 mm, 1 mm and 2 mm, depending on the applied pressure.*

Key Words: *plane-oval cylindrical shell, rigid surface, internal pressure, transverse strain*

1. INTRODUCTION

In most thermoregulatory systems, mainly in cooling or cryogenic plants, cylindrical tubes are used [1]. Their section shape can be rectangular, cylindrical, oval or plane-oval. Similar tubes are used, including, in household, industrial, aircraft and automotive engineering [1], [2], [3], [4], [5], [6]. In particular, there are systems in which, depending on the pressure created, it is necessary to carry out some other heat removal/ supply by controlling the contact zone with the surface [7], [8], [9], [10], [11], [12], [13].

In this work, a similar process is investigated, namely, the study of the contact zone of a plane-oval tube with rigid surfaces at various gaps between them. Such a tube section has a significant advantage over other section shapes and can be easily connected to the flat surfaces of other devices [14], [15], [16], [17]. The mechanical and thermal characteristics of such structures increase due to the higher contact area compared to other section shapes. The investigated plane-oval aluminum shell is installed between two rigid transparent plates [18],

[19], [20], [21]. The shell under consideration with characteristic geometric parameters is shown in Figure 1. The length of the plane-oval shell is 300 mm, the width is $2(l+r) = 60$ mm, and the height is $2r = 2.9$ mm.

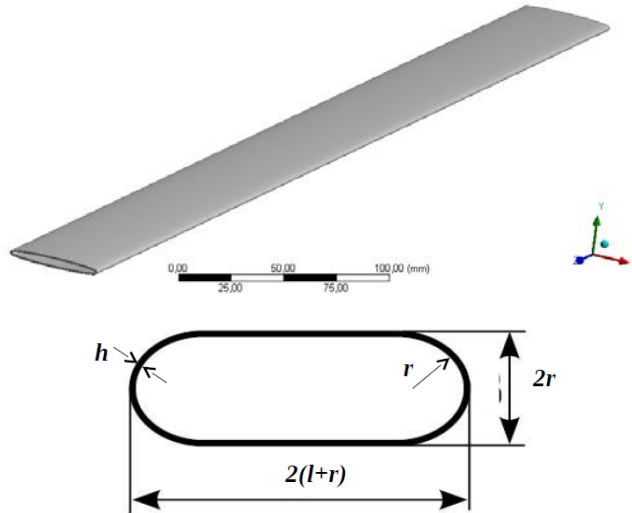


Fig. 1 – Plane-oval tube

The test tube is made of aluminum $E = 71$ MPa, $\nu = 0.3$, and the rigid plates are made of hardened glass with a millimeter scale applied to fix the width of the contact zone. Plane-oval cylindrical shell is subjected to internal pressure varying up to 0.15 atm.

2. EXPERIMENTAL DETERMINATION OF THE CONTACT ZONE WIDTH

To study the width of the contact zone, depending on the gap, a testing workbench was used (Figure 2). The pressure in the tube was supplied from the high-pressure reservoir by fixing the required pressure with a reducer – 6, and the pressure in the tube was fixed with an additional pressure gauge – 5. The set pressure in the plane-oval cylindrical shell was controlled with an accuracy of 0.005 MPa and varied in the range 0 – 0.15 MPa in increments of 0.01 MPa.

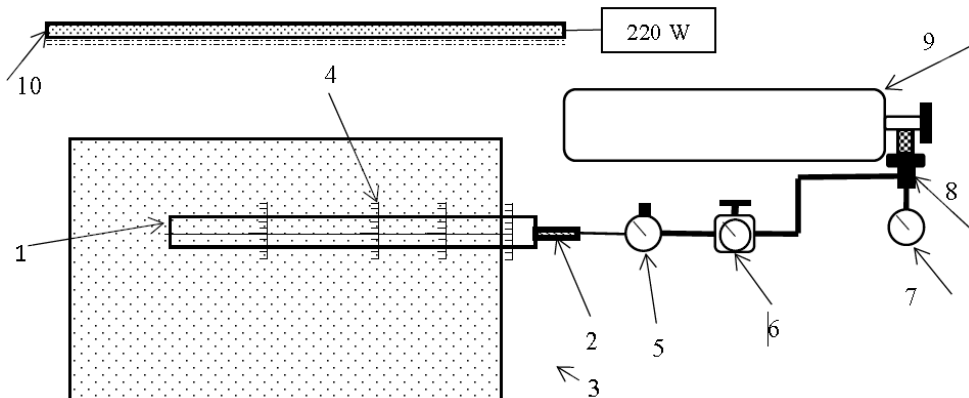


Fig. 2 – Scheme of the testing workbench: 1 - sample; 2 - fitting; 3 - glass; 4 - millimeter scale; 5 - pressure gauge with air reset button; 6 - high-precision pressure-regulating device; 7 - gear monometer; 8 - reducer; 9 - reservoir; 10 - lamp

Contact zone measurement is carried out visually. When pressure is applied, the tube inflates and presses against the glass.

The width of the contact zone can be seen directly on the applied millimeter scales – in the form of shaded areas.

To do this, the backlight is installed and turned on at the end of the glass. For a visual display of contact zones, the pipe surface is pre-coated with liquid wax or water spray.

In this case, when pressurized and being in contact with glass, characteristic bands are formed that allow you to see and measure the contact zone width [1] (Figure 3).

The meniscus size of liquid wax in the gap between the glass and the tube is small and does not significantly affect the measurement results.

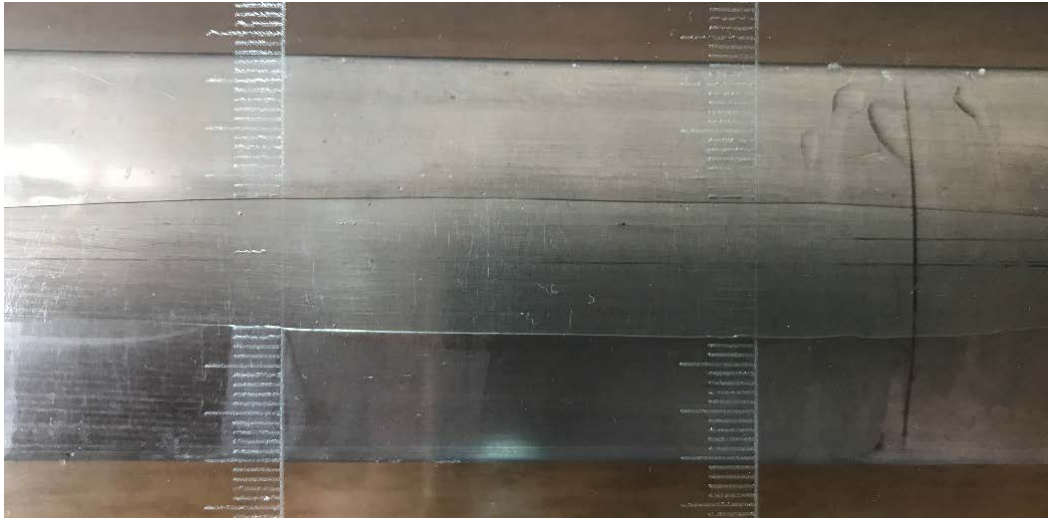


Fig. 3 – The width of the contact zone

The gap between the glasses is set using bolted connections and washers. The gaps are set equal to 0.5 mm, 1 mm, 2 mm. An example of gap is shown in Figure 4.

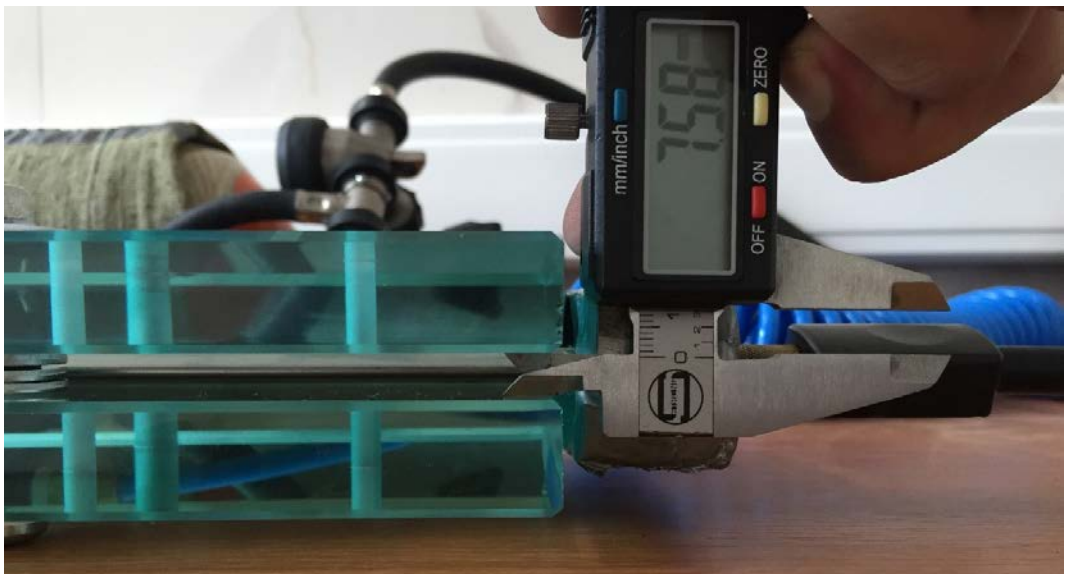


Fig. 4 – Setting the gap between the plates

3. NUMERICAL AND ANALYTICAL MODELING

The problem was solved by the finite element analysis in the Ansys Workbench system. For this, a 1 mm wide plate loaded with distributed pressure was considered (Figure 5).

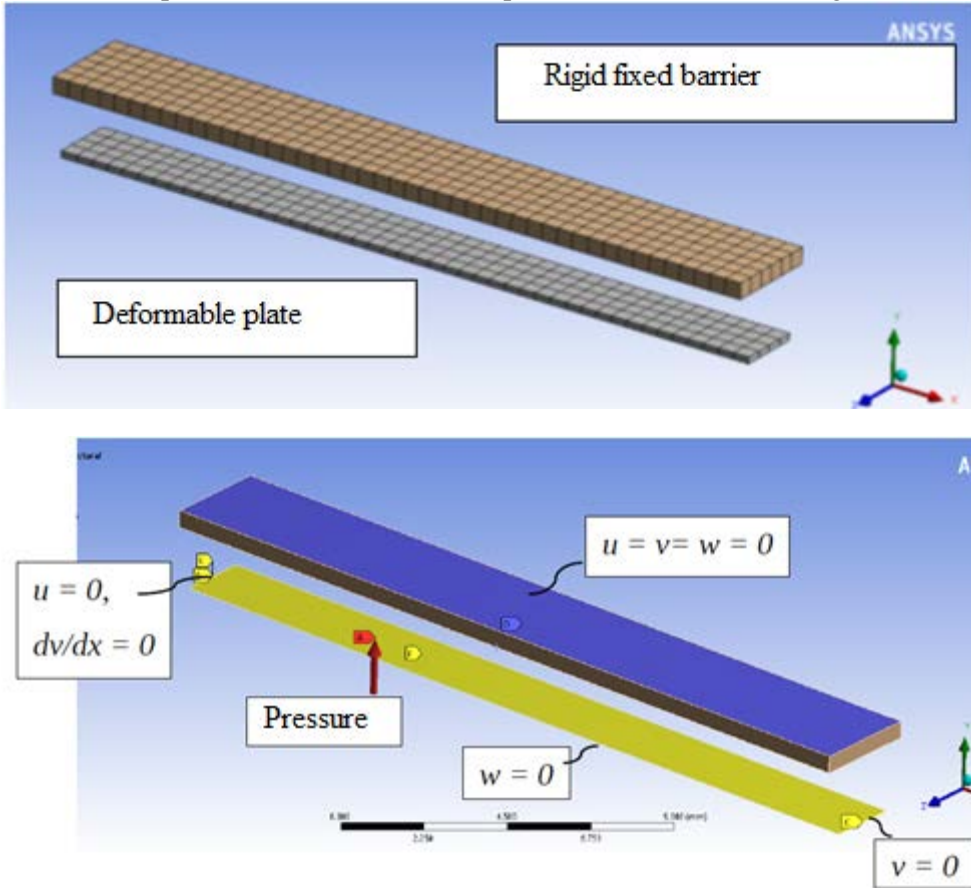


Fig. 5 – Finite-element model and loading scheme in FE calculations for the problem of contact of a plate with a rigid surface under pressure

This plate is actually an element of a plane-oval section of the cooling duct. Symmetry conditions were set at one end of the plate: normal displacements and rotation angles were set equal to zero.

At the other end, zero deflections were set (displacements in the vertical direction). The problem was solved with one-way contact.

A rigid fixed barrier limited from above the movement of the plate. A static calculation was carried out taking into account large deflections [12].

The plate material was set linearly elastic. Contact conditions were set between the plate and the barrier with the initial gap (w) using the modified Augmented Lagrange method, which allows the loss of communication between the contact elements in the calculation process.

Moving the plate in the transverse direction was forbidden to create conditions corresponding to plane deformation. As a result of the calculations, the extent of the contact zone was determined (Figure 6) using the Contact Tool. The size of the grid elements in this figure is 0.5 to 0.5 mm.

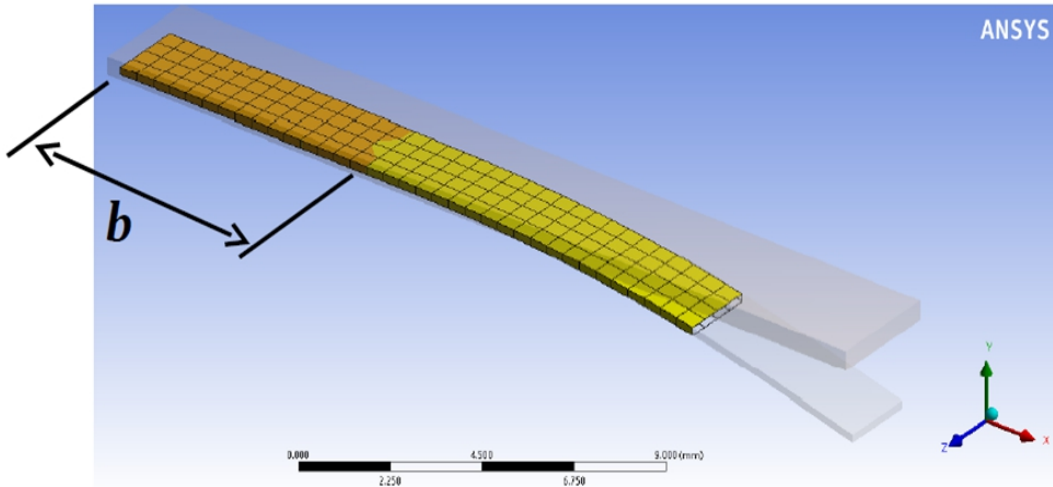


Fig. 6 – An example of the FE calculations results when determining the width of the contact zone.
Orange color – the contact zone of the plate with the barrier

4. THE SOLUTION OF THE PROBLEM

Let us consider the solution of the problem of determining the Timoshenko beam contact zone with a rigid surface under the action of a distributed load and a concentrated force applied at its end. This solution was first obtained also by V. I. Feodosiev [6] for the case of a given value of the concentrated force. In the considered problem, it is necessary to construct a solution for the case of unknown force and a given displacement of the end of the beam.

The Timoshenko beam theory takes into account the shear strain ε_{12} in the beam cross sections and the additional rotations of the beam cross sections φ associated with them [7], [8]. This theory can allow us to refine the solutions for beams (and for plates in the case of a plane deformation problem) of large thickness. The additional inclination of the elastic line caused by the shear is determined by the relation: $\varphi = q/B$, where Q is the shearing force, $B = kGS$ is the beam stiffness in shear, G is the modulus of elasticity in shear, S is the beam cross section area, k is the coefficient, depending on the section shape of the beam in Timoshenko's theory (arises due to the uneven distribution of shear stresses over the beam section), for a rectangular section this coefficient is $k = 5/6$. Note that the cross section of the considered beam – strip has dimensions $1 \times h$ and the area, respectively, is equal to: $S = 1h$.

The beam bowing is determined taking into account bending and shear according to the formula (1):

$$\frac{d^2v}{dx^2} = -\frac{M}{D} + \frac{1}{B} \frac{dQ}{dx} \quad (1)$$

Taking into account the equilibrium equation:

$$Q = \frac{dM}{dx} \quad (2)$$

we obtain:

$$\frac{d^2v}{dx^2} = -\frac{M}{D} + \frac{1}{B} \frac{d^2M}{dx^2} \quad (3)$$

In the beam section, not touching the surface, the moment is determined by the formula:

$$M = p(l - x)^2/2 - F(l - x) \quad (4)$$

We get the equation for determining the deflections in this section:

$$\frac{d^2v}{dx^2} = \frac{1}{D} \left(\frac{p(l - x)^2}{2} - F(l - x) \right) + \frac{p}{B} \quad (5)$$

The deflection function is found by integrating:

$$v = \frac{1}{D} \left(\frac{p(l - x)^4}{24} - \frac{F(l - x)^3}{6} \right) + \frac{px^2}{2B} + C_1 + C_2 \quad (6)$$

The constants C_1, C_2 are determined from the conditions for fixing the cantilever beam at the point $x = b = 1 - a$: $v = 0, \frac{dv}{dx} = 0$.

Solving this system of equations for C_1, C_2 , we find the deflections of the beam outside the contact zone:

$$x \geq b: v = (x - b)^2 \left(\frac{p(3a^2 + 2a(l - x) + (l - x)^2)}{24D} - \frac{F(2a + l - x)}{6D} + \frac{p}{2B} \right) \quad (7)$$

In the area touching the rigid surface, the beam bowing is equal to zero:

$$\frac{d^2v}{dx^2} = \frac{M}{D} - \frac{1}{B} \frac{d^2M}{dx^2} = 0 \quad (8)$$

Solving this equation with respect to the moments, taking into account the boundary conditions $x = 0: M = 0, x = b: M = Fa - pa^2/2$, we find:

$$x \leq b: M(x) = - \left(\frac{pa^2}{2} - Fa \right) \frac{\sinh(x\sqrt{B/D})}{\sinh(b\sqrt{B/D})} \quad (9)$$

In the obtained solution, at the interface point between two sections of the beam (pressed and raised), the condition of equal moments and inclination of the elastic line (this angle is zero) is fulfilled. Equality of movement is easily satisfied due to the arbitrariness in solving the problem for the contacting section of the beam. Thus, the only condition for the equality of the shear strain at the interface point remains, which is used to determine the contact zone width. The shear strain to the right of the point $x = b$ is easily found from the equilibrium condition of this beam section

$$Q|_{x=b+} = pa - F \quad (10)$$

To the left of this point using the resulting formula and the equilibrium equation:

$$Q|_{x=b-} = \frac{dM}{dx} \Big|_{x=b-} \quad (11)$$

We get the relation:

$$Q|_{x=b+} = Q_{x=b-} \Rightarrow pa - F = -(pa^2/2 - Fa)\sqrt{B/D} \operatorname{cth}(b\sqrt{B/D}) \quad (12)$$

The solution of this transcendental equation allows us to find the length of the beam section a , not touching the surface. This solution was obtained in [6], however, it cannot be

used for the problem under consideration, since the magnitude of the force is unknown. It is necessary to determine the relationship of the force F with the value of the specified deflection at the end of the beam $x = 1$. We get:

$$v(l) = \frac{pa^4}{8D} - \frac{pa^3}{3D} + \frac{pa^2}{2B} = w \quad (13)$$

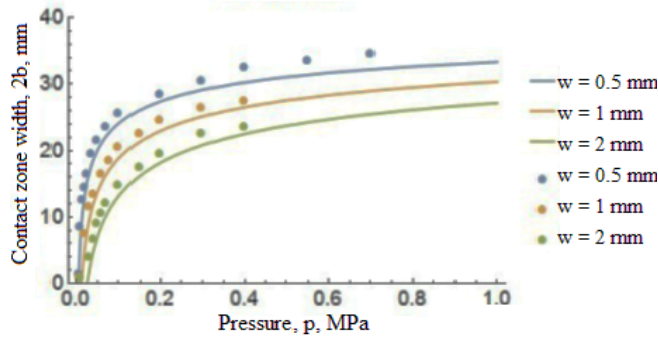
The force acting at the end of the beam:

$$F = \frac{3pa}{8} + \frac{3pD}{2Ba} + \frac{3wD}{a^3} \quad (14)$$

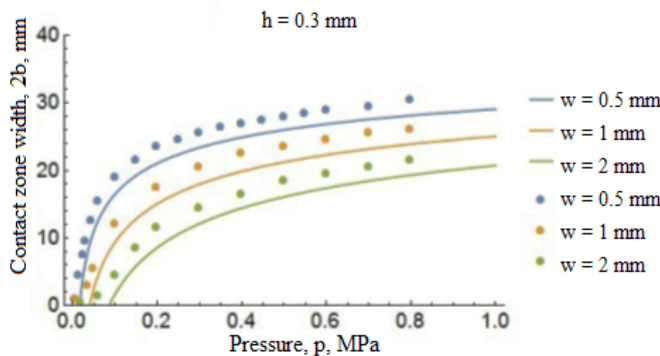
Using the obtained formulas, we find the form of the transcendental equation, the solution of which allows us to find the contact zone width:

$$\frac{3wD}{a^3} + \frac{5pD}{8} + \frac{3pD}{2Ba} = -\sqrt{B/D} \operatorname{cth}((l-a)\sqrt{B/D}) \left(\frac{3wD}{a^2} + \frac{pa^2}{8} + \frac{3pD}{2B} \right) \quad (15)$$

The solution to this transcendental equation was found numerically using the Newton-Raphson method. The length of the segment a was determined from the solution, and the contact zone width was determined as $b = 1 - a$. As a result of experimental, numerical and analytical studies, results were obtained for a plane-oval shell with gaps of 0.5 mm, 1 mm and 2 mm, depending on the applied pressure. A comparison of all the obtained calculations of the contact zone width for different model geometries at different pressure values for a shell thickness of 0.2 mm is shown in Figure 7a. Figure 7b presents a shell thickness of 0.3 mm, and Figure 7c present a shell thickness of 0.5 mm.



a)



b)

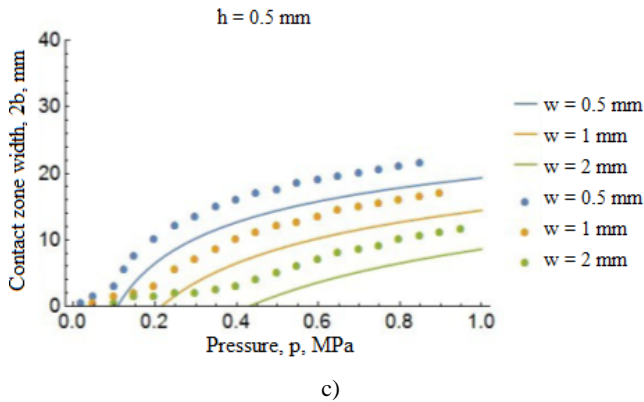


Fig. 7 – Dependence of the contact zone width on pressure and geometric parameters of the problem. The results of analytical calculations in the classical beam theory (line) and numerical calculations (points): (a – for a shell thickness of 0.2 mm, b – for a shell thickness of 0.3 mm, c – for a shell thickness of 0.5 mm)

The deformed state of plates of various thicknesses in contact with the barrier under the action of pressure of 0.1 MPa is shown in Figure 8. The gap was 2 mm. The color in this illustration shows the movement. It can be seen here that visually it is quite difficult to determine the contact zone width from the FE solution (similar effects should be taken into account in experimental studies), and the real contact zone width, in which the surfaces are densely pressed against each other, is less than apparent. This real contact zone width was determined using the Contact Tool in the Ansys system, which works as an indicator and shows the presence of complete coincidence of surfaces in the solution of the problem (Figure 8).

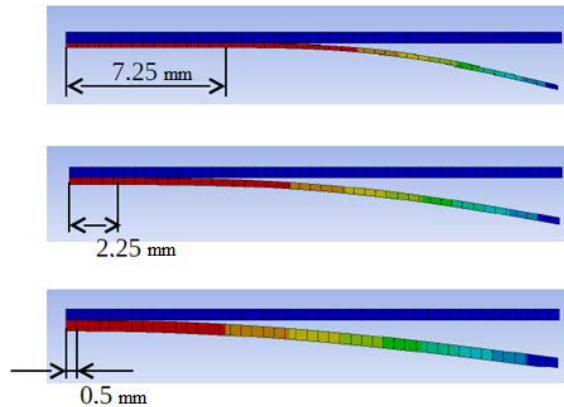


Fig. 8 – Deformed state of plates of various thicknesses. Color shows the deflections of the plate (red – maximum deflection). The contact zone width is determined using the Contact Tool in Ansys

5. CONCLUSIONS

Based on the calculation results, it can be concluded that the obtained relation for estimating the contact zone width is in good agreement with the results of numerical calculations for small plate thicknesses and a small gap. For plates with a relation of length to thickness > 50 , the analytical solution is actually accurate. In this case, the hypotheses of the classical plate theory in the formulations for small deflections are valid. With an increase in the plate thickness and an increase in the gap, the error of analytical calculations with respect to the numerical values increases and amounts to $\sim 30\%$ for plates with a ratio of sizes (length to thickness) of 20-25.

It should also be noted that the numerical solution at high pressures could be quite difficult to converge and require significant time and computational resources even for the simple geometry of the problem under consideration, while the analytical solution allows us to obtain an acceptable, and for thin plates, accurate result. The FE solution, on the contrary, for thin plates converges worse even at low pressures due to the sufficiently large plate movements that occur. Deviation of the FE modeling results from the analytical solution at pressures of more than 0.5 MPa can arise not only due to the analytic error for such loading conditions, but also due to the cumulative errors of FE calculations. To solve this kind of problems, other Ansys modules must be used, designed to solve highly non-linear problems with large deformations (Transient Structural, Autodyn solvers, LS-DYNA).

ACKNOWLEDGMENTS

The work has been conducted with the financial support of the grants of the Russian Foundation for Basic Research (RFBR grant No 20-01-00517A).

REFERENCES

- [1] E. Lomakin, L. N. Rabinskiy and V. Radchenko, Analytical estimates of the contact zone area for a pressurized flat-oval cylindrical shell placed between two parallel rigid plates, *Meccanica*, vol. **53**, no. 15, pp. 3831-3838, 2018. DOI: 10.1007/s11012-018-0919-y.
- [2] Yu. F. Maydanik, M. A. Chernysheva and V. G. Pastukhov, Review: Loop heat pipes with flat evaporators, *Applied Thermal Engineering*, vol. **67**, no. 1/2, pp. 294-307, 2014. DOI: 10.1016/j.applthermaleng.2014.03.041
- [3] E. J. Lee and N. H. Kim, Evaporation heat transfer and pressure drop in flattened microfin tubes having different aspect ratios, *International Journal of Heat and Mass Transfer*, no. 92, pp. 283-297, 2016. DOI: 10.1016/j.ijheatmasstransfer.2015.08.096
- [4] G. G. Adams and M. Nosonovsky, Contact modeling – forces, *Tribology International*, vol. **33**, no. 5, pp. 431-442, 2000.
- [5] R. L. Jackson and J. L. Streater, A multi-scale model for contact between rough surfaces, *Wear*, vol. **261**, no. 11-12, pp. 1337-1347, 2006.
- [6] E. J. Barbero, R. Luciano and E. Sacco, Three-dimensional plate and contact/friction elements for laminated composite joints, *Computers & Structures*, vol. **54**, no. 4, pp. 689-703, 1995.
- [7] V. I. Feodosiev, *Selected tasks and questions on the resistance of materials*, Nauka, 1967.
- [8] L. P. Zheleznov, V. V. Kabanov and D. V. Boyko, Nonlinear deformation and stability of oval cylindrical shells under clean bending with internal pressure, *Applied Mechanics and Technical Physics*, vol. **47**, no. 3, pp. 119-125, 2006.
- [9] L. P. Zheleznov and V. V. Kabanov, Investigation of nonlinear deformation and stability of non-circu, *Applied Mechanics and Technical Physics*, vol. **43**, no. 4, pp. 155-160, 2002.
- [10] A. A. Kolomoets and A. S. Modin, Nonlinear dynamics of a pre-loaded imperfect cylindrical shell under the action of uneven external pressure, *Bulletin of SSTU*, vol. **3**, no. 80, pp. 7-12, 2015.
- [11] A. S. Yudin and D. V. Shchitov, On the calculation of elliptic shells of revolution loaded with internal pressure, *Natural Sciences*, no. 3, pp. 29-36, 2004.
- [12] A. Babaytsev, V. Dobryanskiy and Y. Solyaev, Optimization of thermal protection panels subjected to intense heating and mechanical loading, *Lobachevskii Journal of Mathematics*, vol. **40**, no. 7, pp. 887-895, 2019.
- [13] Y. Solyaev, S. Lurie, A. Koshurina, V. Dobryanskiy and M. Kachanov, On a combined thermal/mechanical performance of a foam-filled sandwich panels, *International Journal of Engineering Science*, no. 134, pp. 66-76, 2019.
- [14] A. A. Skvortsov, D. E. Pshonkin, M. N. Luk'yanov and M. R. Rybakova, Deformations of aluminum alloys under the influence of an additional load, *Periodico Tche Quimica*, vol. **15**, no. 30, pp. 421-427, 2018.
- [15] A. A. Skvortsov, A. M. Orlov and S. M. Zuev, Diagnostics of degradation processes in the metal-semiconductor system, *Russian Microelectronics*, vol. **41**, no. 1, pp. 31-40, 2012.
- [16] V. N. Dobryanskiy, L. N. Rabinskiy and O. V. Tushavina, Experimental finding of fracture toughness characteristics and theoretical modeling of crack propagation processes in carbon fiber samples under conditions of additive production, *Periodico Tche Quimica*, vol. **16**, no. 33, pp. 325-336, 2019.

- [17] L. N. Rabinskiy and O. V. Tushavina, Investigation of the influence of thermal and climate effects on the performance of tiled thermal protection of spacecraft, *Periodico Tche Quimica*, vol. **16**, no. 33, pp. 657-667, 2019.
- [18] Y. Amirgaliyev, M. Kunelbayev, W. Wójcik, B. Amirgaliyev, A. Kalizhanova, O. Auelbekov, N. Kataev and A. Kozbakova, Calculation and selection of flat-plate solar collector geometric parameters with thermosiphon circulation, *Journal of Ecological Engineering*, vol. **19**, no. 6, pp. 176-181, 2018.
- [19] B. A. Antufev, O. V. Egorova and L. N. Rabinskiy, Dynamics of a cylindrical shell with a collapsing elastic base under the action of a pressure wave, *INCAS Bulletin*, vol. **11**, Special Issue, pp. 17-24, <https://doi.org/10.13111/2066-8201.2019.11.S.2>, 2019.
- [20] E. L. Kuznetsova and A. V. Makarenko, Mathematical model of energy efficiency of mechatronic modules and power sources for prospective mobile objects, *Periodico Tche Quimica*, vol. **16**, no. 32, pp. 529-541, 2019.
- [21] S. V. Vasylyuk, A. D. Suprun and V. N. Yashchuk, About possible mechanisms of nanoconductivity in polyenes polymers: The charge solitons at extremely weak external fields, *Springer Proceedings in Physics*, vol. **195**, pp. 187-205, 2017.